Published in final edited form as:
*Brain Imaging Behav*. 2011 December ; 5(4): 295–306. doi:10.1007/s11682-011-9133-4.

# Hemodynamic Responses to Visual Stimulation in Children with Sickle Cell Anemia

**Ping Zou**[1], **Kathleen J. Helton**[1], **Matthew Smeltzer**[2], **Chin-Shang Li**[3], **Heather M. Conklin**[4], **Amar Gajjar**[5], **Winfred C. Wang**[6], **Russell E. Ware**[6], and **Robert J. Ogg**[1]

[1]Department of Radiological Sciences, St. Jude Children's Research Hospital, Memphis, TN

[2]Department of Biostatistics, St. Jude Children's Research Hospital, Memphis, TN

[3]Department of Public Health Sciences, University of California, Davis, CA

[4]Department of Psychology, St. Jude Children's Research Hospital, Memphis, TN

[5]Department of Oncology, St. Jude Children's Research Hospital, Memphis, TN

[6]Department of Hematology, St. Jude Children's Research Hospital, Memphis, TN

## Abstract

Blood oxygenation level- dependent (BOLD) and cerebral blood flow (CBF)-based functional magnetic resonance imaging (fMRI) were used to measure primary visual cortex responses to photic stimulation in 23 children (12.4 ± 0.7 years old) with sickle cell anemia (SCA) and 21 clinical controls (11 ± 1.0 years old). The objectives were to investigate the effect of SCA on detection of brain activation with fMRI and to explore the relationship between fMRI responses and global cognitive function. The BOLD responses were diminished in children with SCA. Clinical indicators of disease severity were greatest in patients without detectable visual cortex activation, but blood hemoglobin concentration and resting CBF were not predictive of BOLD signal amplitude in the SCA patients. Unexpectedly, the BOLD signal amplitude was positively associated ($r_s \geq 0.8$, $p \leq 0.05$) with Wechsler Abbreviated Scale of Intelligence scores, suggesting that fMRI may help clarify medical, hemodynamic, and neural factors that mediate adverse effects of SCA on neurocognitive function.

### Keywords

sickle cell anemia; functional magnetic resonance imaging; brain activation; cognitive function; blood oxygenation level- dependent; cerebral blood flow

## INTRODUCTION

Sickle cell anemia (SCA) is a genetic blood disorder that affects the hemoglobin within the red blood cells. The disease affects millions of people around the world and is most prevalent in those with ancestors from sub-Saharan Africa, India, Saudi Arabia, and Mediterranean countries. As many as 1 in 375 African-Americans is born with sickle cell anemia each year in the United States. The sickle cell hemoglobinopathy is caused by a single nucleotide mutation in the gene coding a major subunit of the hemoglobin molecule. The hemoglobin mutation causes complex molecular and cellular changes, including

Corresponding Author: Robert J. Ogg, PhD, Department of Radiological Sciences, MS 220, St. Jude Children's Research Hospital, 262 Danny Thomas Place, Memphis, TN 38105, Phone: 901-595-2502; Fax: 901-595-3981, robert.ogg@stjude.org.

hemoglobin polymerization that leads to the sickle shape of the red blood cells for which the disease is named. Clinical complications of SCA affect all organs, and are frequently associated with vaso-occlusive and hemolytic manifestations of the disease. With contemporary medical care, which may include chronic red blood cell transfusions or hydroxyurea medication, life expectancy is more than 50 years for patients with SCA and there is keen interest in factors that undermine the quality of life for survivors, including neurocognitive dysfunction.

Children with sickle cell anemia (SCA) suffer cognitive deficits (Bernaudin et al., 2000) that are associated with disease pathophysiology, including elevated cerebral blood volume (CBV) (Steen et al., 1998a) and flow (CBF) (Strouse et al., 2006). The estimated prevalence of vasculopathy (predominantly vessel tortuosity) by magnetic resonance angiography (MRA) is 64% in untreated patients with SCA (Steen et al., 2003). Vessel stenosis and occlusion also develop in some patients. Resting cerebral artery blood velocity and parenchymal CBF may be elevated by 100% in patients with SCA (Oguz et al., 2003; Strouse et al., 2006). Deficits are worse in children with history of cerebrovascular accident or silent infarction by brain MRI, but patients with normal diagnostic MRI can still be impaired and the deficits appear to worsen with age (Wang et al., 2001). Cognitive deficits are also present in otherwise healthy adult patients with SCA (Vichinsky et al., 2010). The fundamental causes of cognitive deficits in SCA without visible evidence of brain injury are unknown.

Functional MRI (fMRI) may be useful to investigate the neural basis of abnormal brain function in SCA patients. Patterns of brain activation are detected with fMRI via hemodynamic changes in the cortex while a subject is receiving sensory stimuli or performing motor or cognitive tasks. In the healthy brain, blood volume and blood flow increase locally in activated cortex (Chen and Ogawa S., 1999; Detre and Alsop, 1999). The blood flow increase is of sufficient magnitude (50 to 80%) that the oxygen extraction fraction decreases and the blood oxygenation increases with activation. Brain activation can be detected with fMRI methods that measure the CBF changes (Detre and Alsop, 1999) or with methods that measure blood oxygenation level dependent (BOLD) signal changes (Ogawa et al., 1990). The BOLD method, which is based on the effect of oxygenation on the magnetic properties of blood hemoglobin (Pauling and Coryell, 1936), is the most widely used because it is the more sensitive method to detect brain activation. With either approach, the detection of activation with fMRI in SCA patients may be compromised by anemia and abnormal cerebral hemodynamics (D'Esposito et al., 2003; Prohovnik et al., 2009; Reiter et al., 2002), even if the neural activity itself was unaffected by disease.

We recently reported resting CBF measurements in a prospectively enrolled cohort of SCA patients, most of whom were receiving hydroxyurea therapy (Helton et al., 2009). The resting CBF, measured by arterial spin labeling (Luh et al., 1999) of these patients was within the upper end of the range of values reported for healthy children. This finding is in contrast to reports of substantially elevated resting CBF in untreated patients with SCA (Oguz et al., 2003; Steen et al., 1998b; Strouse et al., 2006). Here, we report a cross-sectional pilot fMRI study in the same SCA cohort to investigate the effect of SCA on detection of brain activation with fMRI and to explore the relationship between fMRI responses and global cognitive function. We measured the BOLD response (Zou et al., 2005) and CBF response (Detre and Alsop, 1999) in primary visual cortex to simple visual stimulation, and analyzed the fMRI responses in relation to hematologic, rheologic and psychometric variables.

# METHODS

## Subjects

The study was approved by St. Jude Children's Research Hospital Institutional Review Board, and parental consent and patient assent were obtained for all participants. Patients were enrolled prospectively when presenting with various clinical indications, including baseline or serial evaluation on hydroxyurea therapy, deterioration of school performance, or severe headaches. Twenty three pediatric patients with SCA (12.4 ± 0.7 years old, 15 males and 8 females) were enrolled for the fMRI study. Twenty-one of them were on hydroxyurea treatment at the time of fMRI. The enrolled patients had no history of overt stroke and no transfusion within the previous three months. None of the SCA patients had additional conditions, such as epilepsy or traumatic brain injury that would be expected to affect cerebral hemodynamics or brain function.

The original pilot study design did not include a control group. After enrollment and imaging of the SCA cohort was complete, we identified twenty-one age-matched patients (12.3 ± 0.7 years old, 14 males and 7 females) treated at our institution for posterior fossa brain tumor (medulloblastoma) to constitute a comparison group for the BOLD fMRI results. The medulloblastoma patients had participated in another fMRI study using the same visual stimulation paradigm and BOLD fMRI pulse sequence, and they were imaged on the same scanner during approximately the same time period as the SCA group. This cohort had been imaged after successful resection of their tumors (median 19 days, range 3 to 41 days) and prior to radiation therapy (median 3 days, range 0 to 12 days) or chemotherapy (Gajjar et al., 2006).

## Clinical Laboratory and Neuropsychological Testing

Imaging data from children with SCA were analyzed in relation to standard laboratory parameters, including hemoglobin concentration ([Hb]), percent fetal hemoglobin (HbF), absolute reticulocyte count, and incidence of acute chest syndrome events. Testing also included transcranial Doppler ultrasound (TCD) evaluation of blood flow velocity in the middle cerebral artery. Global cognitive function was assessed in 13 children of the SCA group with the Wechsler Abbreviated Scale of Intelligence (WASI) (Wechsler, 1999). Hemoglobin concentration data were also analyzed for the control patients.

## MRI

MRI data were acquired with a 1.5T Siemens Symphony scanner. Two functional data sets were acquired during visual stimulation with the following two MRI pulse sequences. *1) Standard BOLD measurement:* a T2*-weighted echo planer imaging (EPI) sequence with TR = 2060 ms, TE = 50 ms, bandwidth = 1954 Hz/Pixel, matrix = 64 × 64, FoV = 192 mm, slice thickness = 5 mm, and flip angle = 90° was used. Twenty-three slices with full brain coverage and 135 image (voxel size 3×3×5 mm) volumes were acquired. *2)* arterial spin labeling (ASL) *CBF measurement:* a pulsed ASL Q2TIPS sequence (Luh et al., 1999) with TR = 2200 ms, TE = 26 ms, TI1 = 700 ms, TI1s = 1200 ms, TI2 = 1400 ms, bandwidth = 2170 Hz/Pixel, matrix = 64 × 64, FoV = 192 mm, slice thickness = 7.5 mm, and flip angle = 90° was used. Four slices covering the occipital lobe and 174 image (voxel size 3×3×7.5 mm) volumes were acquired. The BOLD response was also estimated from the ASL data, but the ASL-based measurement is less sensitive than the standard method. In addition to the functional images, standard fluid-attenuated inversion recovery (FLAIR), T1, T2, and proton density images were acquired for conventional MRI evaluation, segmentation, and co-registration with functional images.

As an index of cerebral blood volume (Steen et al., 1998a; Steen et al., 1998b), the apparent diameter of the basilar artery was measured at the level of the mid-pons on FLAIR images. The parameters of the FLAIR pulse sequence were TR = 91400 ms, TE = 112 ms, TI = 2400 ms, matrix = 192 × 256, FoV = 157.5 × 210 $mm^2$, slice thickness = 5 mm, and acquisitions = 2. The diameter was measured with standard tools on the institutional picture archiving and communication system (Siemens Syngo). Images were zoomed by a factor of 3 and the display intensity center value was 500 and the display intensity window was 1000. Images showing the basilar artery diameter measurement for the participants with the median value for each group are shown in the supplemental information (Supplemental Fig. 1).

## Visual stimulation for fMRI

The visual stimulus was a black and white checkerboard with color reversal at 8 Hz. One stimulation paradigm included visual stimuli of brief and long duration, and was presented to both the SCA and tumor control cohorts during the standard measurement of BOLD responses. The stimulation paradigm had four 30 sec blocks in which stimulus was on for 2 sec (BOLD_2s) and three 40 sec blocks in which the stimulus was on for 16 sec (BOLD_16s). This paradigm was 4 min long. A similar stimulation paradigm with eight 40 sec blocks, each with stimulus on for 20 sec, was used in the SCA cohort during the simultaneous measurement of CBF and BOLD changes with the pulsed ASL technique. The ASL fMRI paradigm was 5 min 20 sec long. These kinds of visual stimulation paradigms are know to elicit strong brain activation in primary visual cortex (Deyoe et al., 1994; Zou et al., 2005). The brain tumor control group was drawn from another study protocol that did not include ASL fMRI.

## Analysis of functional images

SPM2 (http://www.fil.ion.ucl.ac.uk/spm/) was used in image preprocessing and statistical analysis of the functional images and MarsBar toolbox for SPM was used in retrieving time-course of raw data from regions of interest (ROI). The thresholds for estimating activation volume and retrieving time-course data were $p = 0.001$ (uncorrected) for SPM voxel height and $k = 5$ voxels ($p < 0.01$ uncorrected) for spatial extent, unless otherwise noted.

**Standard BOLD fMRI—**Functional images for each subject were first visually inspected to exclude those with unacceptable quality, such as susceptibility distortion caused by brain shunt. Then images were realigned to correct head motion. Preprocessed images were analyzed using a general linear model (GLM) with a covariate of interest modeling the BOLD response signal as the convolution of the time-course of the stimulation paradigm and the canonical HRF (Friston et al., 1998). Statistical contrasts were evaluated to detect greater activity during stimulation than during fixation (brain activation to visual stimuli) and greater activity during fixation than during stimulation (brain activation during rest – default mode network). Brain activation volume for the SCA group was obtained and compared to the volume for brain tumor control group using the Wilcoxon-Mann-Whitney (W-M-W) Test. The spatial location of activation was determined by visual comparison to the Talairach Atlas for each subject. The time-course of the peak activation region in the primary visual cortex (V1) was retrieved and adjusted to percentage BOLD signal change over the blocks for each subject. The final BOLD signal for the brief stimulus or the long stimulus for each subject was a block-wise average over the corresponding blocks. Repeated measures ANOVA (Mixed procedure in SAS software, V9, SAS Institute Inc., Cary, NC, USA) was used to test for difference between the SCA and brain tumor groups in the BOLD signal amplitude over time.

**ASL images—**To maximize the efficiency and power of the functional analysis of the ASL time-series data, a GLM modeling the full data set was used (Mumford et al., 2006).

The GLM included three covariates of interests. The first covariate modeled the baseline variation of image intensity due to the alternation of control and tag states when no stimulation is presented. It consisted of a vector with values of 0.5 and −0.5 corresponding to control and tag conditions. The second covariate modeled the BOLD signal component and was set up as the convolution of stimulation paradigm and the canonical HRF. The third covariate modeled the activation component of the control-tag difference signal (CBF activation) during the visual stimulation and was formed by modulating the BOLD response with the control-tag condition. Brain activation volume for BOLD and CBF were obtained at various thresholds. The activation pattern of BOLD and CBF were visually compared. Raw ASL time-courses from the overlapping region of CBF and BOLD activation were retrieved. A tag signal was calculated from ASL raw time-course as the average of the previous and the next time-points of each control time-point so that it was insensitive to linear trends in the data (Wong et al., 1997). The BOLD signal was obtained as the average of the control and the tag signals at each time point. A differential time-course, representing the CBF signal, was calculated by subtracting the tag signal from the control signal at each time point. The BOLD signal was adjusted to percentage change and used to calculate the group average of BOLD responses. The differential signal was used to quantify absolute CBF values.

## Quantification of CBF

For each subject, CBF was quantified from the differential signal or images ($\Delta S$) as described by Luh (Luh et al., 1999):

$$CBF = \Delta S \frac{L}{2M_{0_{blood}} \cdot A \cdot TI1 \cdot e^{-TI2/T1_{blood}}}$$

where the values used are: $L = 90\ mL/100g$, $A = 0.95$, and $T1_{blood} = 1.2\ sec$. To estimate the fully relaxed magnetization $M_{0blood}$ of arterial blood, ASL images acquired with another Q2TIPS sequence with the same parameters except shorter TE ($TE = 13ms$) was included to estimate $T2^*$ of blood using equation:

$$\frac{S_{b1}}{S_{b2}} = \frac{e^{-TE_1/T2^*_{blood}}}{e^{-TE_2/T2^*_{blood}}}$$

where $S_{b1}$ or $S_{b2}$ was the corresponding raw EPI intensity at the given TE. Then $M_{0blood}$ was estimated as raw EPI intensity scaled to $TE = 0$ and $TR = infinite$ according to:

$$S_b = \frac{M_{0_{blood}} \cdot (1 - e^{-TR/T1_{blood}}) \cdot \sin(\theta) \cdot e^{-TE/T2^*_{blood}}}{(1 - \cos(\theta)) \cdot e^{-TR/T1_{blood}}}$$

where the flip angle θ = 90°.

## Gray and white matter CBF values for the whole brain and occipital lobe

A perfusion weighted image (PWI) was produced that was the average of the tag-control (Wong et al., 1997) differential images from the ASL series for each subject. The T2-

weighted anatomical image was segmented with SPM2. Gray and white matter masks were generated from the corresponding segmentation probability images with a 0.75 probability threshold. The ASL and T2-image were co-registered with SPM2 so that the gray or white matter masks could be applied to the PWI image to create a segmented PWI image (gray matter PWI image or white matter PWI image). Finally, the segmented PWI image was used in the CBF quantization to produce a gray or white matter CBF image. The mean gray and white matter CBF values for the whole brain were obtained from these CBF images. Region-of-interest (ROI) of the occipital lobes was drawn, and the gray and white matter CBF values for the occipital lobes were calculated for each SCA patient.

## Statistical analysis

For the SCA cohort, statistical analysis was performed to evaluate relationships among the imaging results, clinical data, and cognitive testing data. Since many of the variables were not normally distributed (Shapiro-Wilk test), the non-parametric Spearman's Rank Order Correlation Coefficient ($r_s$) was used to investigate the association between pairs of these variables. All analyses were conducted in an exploratory manner. The Holm's procedure, a sequentially rejective procedure that will maintain an experiment-wise error rate of 0.05, was used to calculate p-values adjusted for multiple comparisons. Finally, the SCA cohort was categorized in 2 ways: 1) with or without visual cortex activation detectable by standard BOLD measurement, 2) normal (≤170 cm/s) or conditionally high (171 to 199 cm/s) TCD blood velocity (Bulas, 2005). The results of CBF measurement, cognitive tests, and clinical tests were compared between the categories using the Wilcoxon-Mann-Whitney Test (W-M-W) with exact p-values. Fisher's Exact Test was used to compare categorical variables.

## BOLD signal model

The balloon model (Buxton et al., 2004) was used to characterize the BOLD response to visual stimulation for SCA and control patients. The model includes several physiological parameters (Buxton et al., 2004) likely to be affected by SCA, including transit time, oxygen extraction fraction, blood flow change during activation, the relationship between flow and volume in the cerebral vasculature, and vessel elasticity. The balloon model relates the BOLD signal measured with MRI to the dynamic changes of blood volume, $v(t)$, and deoxyhemoglobin concentration, $q(t)$, in the cerebral vasculature during activation:

$$\frac{d}{dt}q(t)=\frac{f(t)}{\tau_{MTT}}\left(\frac{E(t)}{E_0}-\frac{q(t)}{v(t)}\right)+\frac{1}{\tau_V(t)}\left(f(t)-v(t)^{\frac{1}{\alpha}}\right)\frac{q(t)}{v(t)}$$
$$\frac{d}{dt}v(t)=\frac{1}{\tau_V(t)}\left(f(t)-v(t)^{\frac{1}{\alpha}}\right)$$

where f(t) is the CBF normalized to baseline, E(t) is oxygen extraction fraction, $E_0$ is the baseline oxygen extraction fraction, $\alpha$ the exponent of the steady state flow-volume relationship ($v = f^{\alpha}$), $\tau_{MTT}$ is the transit time through the vascular balloon, and $\tau_v(t)$ is the viscoelastic time constant of the vascular balloon. The viscoelastic time constant is modeled with one value for inflation ($\tau_+$) and another value for deflation ($\tau_-$). The BOLD signal is calculated from $q(t)$ and $v(t)$:

$$BOLD(t)=V_0[Hb](k_1(1-q(t))+k_2(1-v(t)))$$

where $BOLD(t)$ is the BOLD signal normalized to baseline, $V_0$ is the resting venous blood volume, [Hb] is the relative hemoglobin concentration, and k1 and k2 are constants that depend on experimental and physiological parameters.

We modeled the group average time courses for both brief and long stimulus conditions and the individual participant time courses for the long stimulus condition. The Balloon Model is over-parameterized, so we used measured values when available (e.g., hemoglobin concentration, CBF response in the SCA group) and relevant values from the literature when appropriate (e.g., blood volume in SCA group relative to the control group). A fixed functional form of the CBF time course was used for modeling, and was based on the mean measured response from the SCA patients for the long stimulus. A simple ramp function was used for the brief stimulus. The amplitude of the CBF change during activation was the measured value for the SCA group and was varied to achieve a good model fit for the control group. During fitting, the changes in CBF and oxygen extraction were constrained to correspond to a 20% change in oxygen metabolism. We modeled the group average responses first, and then used the model parameters for the group as starting values for fitting the individual responses. Additional details of the BOLD signal modeling are provided in the supplementary online material (See supplementary online material).

## RESULTS

The clinical laboratory, imaging, and psychometric parameters for the participants are summarized in Table 1. All the data were reported in median (min, max) format. None of the SCA patients had visible stenosis by MRA. Conventional MRI findings were non-significant for all the SCA patients except three with minor abnormality (two leukoencephalopathy and one punctate hemosiderin) and none of these abnormalities involved the occipital lobes.

### Brain activation detected with standard BOLD fMRI

The fraction of patients with detectable primary visual cortex activation at the given thresholds, the magnitude of BOLD signal changes, and the volume of activated brain detected with standard BOLD fMRI were lower in patients with SCA than in the medulloblastoma controls (Figure 1 and Figure 2). BOLD activation in the primary visual cortex was detected in 17 (74%) of the 23 SCA patients and in all of the 21 control patients. No activation was detected in the two SCA patients who were not on hydroxyurea therapy. The volume of visual cortex activation was significantly lower (p=0.0005) in SCA patients (5.5 (0.23, 20.2) $cm^3$) than in the brain tumor controls (19.1 (1.3, 48.5) $cm^3$). In addition, 5 (24%) brain tumor controls, but none of the SCA patients, had detectable activation of the default mode network during the resting periods of the stimulation paradigm that included the posterior cingulate and lateral parietal cortex (Binder et al., 1999). The brain activation volumes for the 3 patients with abnormality on MRI were 5.58, 1.8, and 0.23 $cm^3$.

The amplitude of the BOLD signal detected during visual stimulation was significantly lower ($p = 0.006$ for the brief 2-s and $p = 0.025$ for the long 16-s) in SCA patients than in medulloblastoma controls. The group average BOLD signal for both groups to the brief 2-s or the long 16-s stimulation had typical BOLD signal characteristics (Figure 2). However, the temporal dynamics of the BOLD response to activation were different in SCA patients than in controls. Repeated measures ANOVA revealed significant group by time interaction effects for BOLD signals for both the brief and long stimulation. For the brief stimulus, the differences were significant at the peak of BOLD signal change from 6 to 8 s after stimulus onset ($p = 0.006$). For the long stimulus, the differences were significant at the peak starting at 6 s and continuing until 18 s after stimulus onset ($p < .03$).

### ASL fMRI in SCA patients

We were able to acquire ASL data in 22 of the 23 SCA patients. With statistical threshold p=0.05 and k = 5, activation was detected in 19 SCA patients by both BOLD and CBF changes (Figure 3). The time-course of BOLD and CBF changes from overlapped clusters of

activation in visual cortex are also shown in Figure 3. During stimulation, the average BOLD signal amplitude increased 2.9% while CBF increased 62% (from 73.8 (16.6, 132.1) to 119.5 (22.3, 213) ml/min/100g). Table 1 shows the baseline CBF estimated from the ASL data for the whole brain and for the occipital lobe. The CBF values of gray matter and white matter were significantly correlated ($r_s = 0.73$, $p < 0.0001$), but not correlated with baseline CBF in the activated clusters, the BOLD signal amplitude, percentage CBF change during activation, or the volume activated. The overall occipital lobe CBF was higher than in other brain regions; but the baseline CBF in the activated cortex (73.8 (16.6, 132.1) ml/min/100g) was lower than the overall occipital gray matter average (92.3 (26.6, 150.8) ml/min/100g). The CBF change during activation detected with ASL was associated ($p = 0.048$) with the BOLD signal change during the long stimulus measured with the standard BOLD fMRI.

## BOLD signal Model

The Balloon Model (Buxton et al., 2004) yielded a good fit to the BOLD responses for the 2-s and 16-s stimuli for both groups. (Figure 2 and Figure 3) (See supplementary online material). The model results demonstrated that the altered BOLD response in SCA patients can be accounted for by changes in physiological parameters that are consistent with known pathology for this disease (Table 2). The [Hb] in this hydroxyurea-treated SCA group was 34% lower then the control group, with the control group in the normal range. The modeled change in flow was 17% lower and the change in oxygen extraction was 28% lower in the SCA group. The flow-volume parameter, $\alpha$, was elevated 20% and transit time was elevated 50% in SCA patients. The viscoelastic time constants were lower in the SCA patients. The model was able to accommodate the range of BOLD responses observed in both groups with fidelity to the major features of the responses (Supplemental Fig 2). The parameters varied over a narrow range around the group median to achieve reasonable fits to individual BOLD time courses (Table 2). The maximum BOLD signal change was driven primarily by the changes in flow and oxygen extraction, which were, in turn, associated with hemoglobin and blood volumes variation across subjects (Supplemental Fig. 2). The minimum BOLD signal during the post-stimulus undershoot was not clearly associated with the maximum, and was affected most strongly by the viscoelastic time constant, $\tau_-$ (Supplemental Fig. 3).

## Correlations among fMRI, clinical, and cognitive testing results in the SCA patients

Overall, the BOLD signal amplitude was significantly associated both the Hb ($r_s = 0.71$, $p < 0.00001$) and basilar artery diameter ($r_s = -0.44$, $p=0.004$) (Figure 4). The Hb and HbF levels were significantly higher ($p = 0.01$ and 0.03, respectively) and the absolute reticulocyte count significantly lower ($p = 0.01$) in the SCA patients with detectable activation than in those SCA patients without detectable activation (Table 3). In SCA patients with detectable visual activation, the volume activated was inversely correlated with absolute reticulocyte count ($r_s = -0.73$, $p = 0.01$). For the standard BOLD measurement, the BOLD signal amplitude was not strongly associated with hematologic and hemodynamic variables, Hb, HbF, CBF, or Basilar Diameter for SCA patients. Remarkably, there was significant correlation between the BOLD_2s signal amplitude and the WASI Verbal score ($r_s = 0.85$, $p = 0.04$) and between the BOLD_16s signal amplitude and the WASI Performance score ($r_s = 0.82$, $p = 0.05$). Before adjustment for multiple comparisons, the BOLD_16s was also marginally associated with the WASI Verbal score ($p = 0.07$) and the BOLD signal amplitude measured with the ASL sequence was marginally associated with the WASI Performance score ($p=0.066$). The WASI scores were low for the SCA patients without detectable activation. Figure 5 shows the strong association between WASI Full-Scale and the BOLD response to visual stimulation in the patients with SCA, with the BOLD amplitudes for patients without detectable activation set to zero (gray symbols) because their activation was not statistically different from zero. The WASI Verbal score

was associated with HbF ($r_s = 0.76$, $p = 0.02$). There was no significant association between WASI scores and CBF or other the clinical variables evaluated.

## DISCUSSION

The BOLD signal in the brain reflects metabolic and hemodynamic responses to changes in neural activity. In activated cortex, increased cerebral metabolic rate of oxygen and glucose is sustained by increased CBF and CBV (Buxton et al., 1998; Mandeville et al., 1998). In the healthy brain, the oxygen extraction fraction decreases with increased CBF, and therefore blood oxygen saturation increases and deoxyhemoglobin concentration decreases. The fundamental mechanisms that mediate the neural-hemodynamic coupling in the brain are not well understood, but it has been proposed that increased blood oxygen concentration is needed in the activated cortex to increase the diffusive flux of oxygen from the capillaries to the mitochondria (Buxton and Frank, 1997). The MRI signal is sensitive to blood oxygenation changes because the magnetic properties of hemoglobin change with oxygenation (Pauling and Coryell, 1936) such that oxyhemoglobin is essentially nonmagnetic and deoxyhemoglobin is paramagnetic. Decreased deoxyhemoglobin in the activated cortex causes an increase in the BOLD MRI signal (Chen and Ogawa S., 1999). Several pathophysiological features of SCA can affect the BOLD response to neural activation, including anemia, elevated resting CBV and CBF, and decreased vessel elasticity.

This study was motivated by the idea that altered resting CBF and CBV in SCA patients may diminish the BOLD response because of limited capacity to increase CBF in response to increased neural activity. In the healthy adult, the BOLD response is reduced (about 20%) with the global increase of baseline CBF (about 50%) induced by breath holding, breathing $CO_2$, or injection of acetazolamide, while the CBF change with task activation remains about the same despite elevation of the baseline (Brown et al., 2003; Davis et al., 1998; Kastrup et al., 1999). Baseline CBF is often much higher than normal in patients with SCA (Oguz et al., 2003; Steen et al., 1998b; Strouse et al., 2006) to maintain oxygen delivery to the brain.

In our SCA cohort, the middle cerebral artery blood velocity (TCD) and occipital GM perfusion were at the upper end of the normal range (Helton et al., 2009), but the resting CBF in the activated cortex was lower than the overall occipital lobe average resting CBF. The CBF increase with activation was 62% in our SCA patients (Figure 3), which is lower than the 70 to 90% changes that have been reported for comparable visual stimulation experiments in healthy adults (Leontiev and Buxton, 2007). However, the BOLD signal amplitude was not strongly associated with the resting CBF. The lack of association of BOLD signal with resting CBF may reflect important physiological effects of SCA on the BOLD signal mechanism, but these findings must be interpreted cautiously because of the limitations of the accuracy and sensitivity of multislice pulsed-ASL method for CBF quantification. Further studies will be needed to clarify the relationship between BOLD response and resting CBF in SCA patients, including untreated SCA cohorts that will likely have much higher resting CBF (Oguz et al., 2003; Steen et al., 1998b; Strouse et al., 2006).

Abnormal blood hemoglobin concentration and CBV can affect the BOLD response in SCA patients because the BOLD signal depends on the total amount of deoxyhemoglobin in the volume of tissue represented by the image volume element (voxel). Other factors being equal, anemia would reduce the BOLD signal from activated cortex because the amount of hemoglobin in the blood is less than normal. The percentage change in the BOLD signal is correlated with baseline hematocrit in healthy subjects, but the activation volume is not (Gustard et al., 2003; Levin et al., 2001). Over all participants in our study, BOLD signal

amplitude was associated with blood hemoglobin concentration. The SCA patients with detectable V1 activation had significantly higher hemoglobin and fetal hemoglobin levels and significantly lower absolute reticulocyte count than those without detectable V1 activation. Therefore, the low blood hemoglobin level in our SCA cohort at least partially accounts for the low BOLD signal in these patients. However, the BOLD signal was not correlated with hemoglobin concentration within the SCA group. This observation may be accounted for in part by the elevated CBV in the SCA group, such that total hemoglobin in a voxel was not as low as hemoglobin concentration would suggest, and flow and volume interact to determine the BOLD signal during activation. In addition, the differences of temporal dynamics of the BOLD response in the SCA patients (Figure 2) could be related to changes in the elastic (Manci E et al., 1996) or vasomotor (French et al., 1997) properties of the cerebral vasculature that affect both the steady-state and the dynamic relationship between flow and volume (Buxton et al., 1998). Our modeling of the data supported that differences in the BOLD response temporal pattern between SCA and control patients could be accounted for by differences in blood hemoglobin concentration, CBF responses, and changes in oxygen extraction fraction during stimulation, CBV, and mechanical characteristics of the cerebral vasculature. Therefore, the BOLD response in an individual patient may be modulated by different adaptive vascular responses to anemia.

The BOLD responses we report were affected by hydroxyurea therapy in most patients in the SCA cohort. Hydroxyurea therapy is an alternative to blood transfusion in patients at risk for stroke, which reduces resting CBF and increases fetal hemoglobin (Heeney and Ware, 2008; Ware et al., 1999). In our SCA cohort, the resting CBF was not elevated as reported in other patients with SCA (Oguz et al., 2003; Strouse et al., 2006), likely because of hydroxyurea therapy (Ware et al., 1995). The effect of resting CBF was discussed above, and we know of no studies that have characterized the effect of elevated fetal hemoglobin on the BOLD signal. Fetal hemoglobin has higher oxygen affinity than adult hemoglobin, which could affect the change in oxygen extraction fraction during activation that is a key factor in the BOLD signal. Indeed, in our balloon model the change in oxygen extraction fraction during visual stimulation was lower in the patients with SCA than in the controls. On the other hand, fetal hemoglobin was much lower in the SCA patients without detectable BOLD signal and the WASI Verbal score was positively associated with HbF. Prospective longitudinal neuroimaging studies with evaluations prior to hydroxyurea treatment are needed to clarify the effects of this important therapy on cerebral hemodynamics and brain function in patients with SCA.

Cognitive deficits in SCA patients are well documented (Berkelhammer et al., 2007; Schatz et al., 2002), but the cause of the deficits is unknown, especially in children with no imaging evidence of cerebrovascular events (stroke, silent infarct). Decline in IQ has been associated with hematologic abnormalities, including anemia, elevated CBV, and elevated CBF (Bernaudin et al., 2000; Hogan et al., 2006; Steen et al., 2003a; Strouse et al., 2006). These hematologic abnormalities were observed in our SCA patients, but were not individually correlated with psychometric measures of global cognitive function. The strong association that we observed between the BOLD response to simple visual stimulation and WASI scores suggests that the adverse effect of SCA on brain function is mediated by the inability to mount an appropriate hemodynamic response to support increased neural activity (Moore and Cao, 2008). The fact that global intelligence scores were related to the BOLD response to simple sensory stimulation suggests that visual cortical response is an indicator of a globally affected response in the SCA patients.

Our comparison of the BOLD response in the SCA patients to a cohort of patients being treated for medulloblastoma, rather than to typically developing children, had both disadvantages and advantages for this study. The brain tumor patients were studied after

tumor resection, but before any radiation therapy or chemotherapy. It is likely that brain homeostasis and function were adversely affected by presurgical tumor development and growth (Gibson et al., 2010; Ohm and Carbone, 2002; Salsman et al., 2011) and postsurgical edema, tissue compression, apoptosis, or white matter alteration (Morris et al., 2009). The facts that the medulloblastoma patients had blood hemoglobin concentration in the normal range, and their BOLD response to the brief visual stimulus was essentially the same as the response that we reported previously for an age similar cohort (12.1 ± 0.9 yrs, range 8 to 16) of healthy children (Zou et al., 2005a; Zou et al., 2005b) suggest that the data from brain tumor patients are useful to calibrate our measurements in the SCA patients. Furthermore, comparison with medulloblastoma patients helps to control for potential effects of frequent hospitalizations, immune dysfunction, family stress, and other illness-related factors. Finally, our findings demonstrate an important neurobiological deficit in SCA patients relative to another abnormal population that suffers long-term cognitive disability (Mulhern et al., 2004), which strengthens the results of this study.

The findings in this study must be interpreted with consideration of two important limitations. First, the small sample size and large number of variables under consideration limited our power to detect small effects. This problem was most severe for the group of SCA patients without detectable visual cortex activation (n = 5). Second, the SCA group included three patients with evidence of brain injury on conventional imaging. The abnormalities were classified as minor by our neuroradiologist (KJH) and none directly affected the occipital lobes.

Despite these limitations and whatever the exact cause of the abnormal BOLD responses in patient with SCA, our finding demonstrates that it is functionally significant. An interesting hypothesis to test in the future is that some cerebral adaptive responses to chronic anemia (e.g., changes in CBF, CBV) are better than others to preserve cognitive function of the brain. Further characterization of the relationship between hemodynamic and neural responses in SCA may provide important new insights into the causes of cognitive deficits associated with this disease and help to clarify the critical role that cerebral hemodynamics play in information processing in the human brain (Moore and Cao, 2008).

## Supplementary Material

Refer to Web version on PubMed Central for supplementary material.

## Acknowledgments

This work was supported in part by grants from the National Institutes of Health (U54HL70590 (NHLBI), P30CA21765 (NCI), R01HD049888 (NICHD)) and by the American Lebanese Syrian Associated Charities (ALSAC). We thank the anonymous reviewers for their many valuable insights and suggestions to improve the significance and quality of this paper.

## Reference

Berkelhammer LD, Williamson AL, Sanford SD, Dirksen CL, Sharp WG, Margulies AS, Prengler RA. Neurocognitive sequelae of pediatric sickle cell disease: a review of the literature. Child Neuropsychol. 2007; 13:120–131. [PubMed: 17364569]

Bernaudin F, Verlhac S, Freard F, Roudot-Thoraval F, Benkerrou M, Thuret I, Mardini R, Vannier JP, Ploix E, Romero M, Casse-Perrot C, Helly M, Gillard E, Sebag G, Kchouk H, Pracros JP, Finck B, Dacher JN, Ickowicz V, Raybaud C, Poncet M, Lesprit E, Reinert PH, Brugieres P. Multicenter prospective study of children with sickle cell disease: radiographic and psychometric correlation. J.Child Neurol. 2000; 15:333–343. [PubMed: 10830200]

Binder JR, Frost JA, Hammeke TA, Bellgowan PS, Rao SM, Cox RW. Conceptual processing during the conscious resting state. A functional MRI study. J Cogn Neurosci. 1999; 11:80–95. [PubMed: 9950716]

Brown GG, Eyler Zorrilla LT, Georgy B, Kindermann SS, Wong EC, Buxton RB. BOLD and perfusion response to finger-thumb apposition after acetazolamide administration: differential relationship to global perfusion. J.Cereb.Blood Flow Metab. 2003; 23:829–837. [PubMed: 12843786]

Bulas D. Screening children for sickle cell vasculopathy: guidelines for transcranial Doppler evaluation. Pediatr.Radiol. 2005; 35:235–241. [PubMed: 15703903]

Buxton RB, Frank LR. A model for the coupling between cerebral blood flow and oxygen metabolism during neural stimulation. J.Cereb.Blood Flow Metab. 1997; 17:64–72. [PubMed: 8978388]

Buxton RB, Uludag K, Dubowitz DJ, Liu TT. Modeling the hemodynamic response to brain activation. Neuroimage. 2004; 23(Suppl 1):S220–S233. [PubMed: 15501093]

Buxton RB, Wong EC, Frank LR. Dynamics of blood flow and oxygenation changes during brain activation: the balloon model. Magn Reson.Med. 1998; 39:855–864. [PubMed: 9621908]

Chen, W.; Ogawa, S. Principle of BOLD-functional MRI. In: Moonen, CTW.; Bandettini, PA., editors. Functional MRI. Berlin: Springler-Verlag; 1999. p. 103-113.

D'Esposito M, Deouell LY, Gazzaley A. Alterations in the BOLD fMRI signal with ageing and disease: a challenge for neuroimaging. Nat.Rev.Neurosci. 2003; 4:863–872. [PubMed: 14595398]

Davis TL, Kwong KK, Weisskoff RM, Rosen BR. Calibrated functional MRI: mapping the dynamics of oxidative metabolism. Proc.Natl.Acad.Sci.U.S.A. 1998; 95:1834–1839. [PubMed: 9465103]

Detre, JA.; Alsop, DC. Perfusion fMRI with arterial spin labeling (ASL). In: Moonen, CTW.; Bandettini, PA., editors. Functional MRI. Berlin: Springler-Verlag; 1999. p. 47-62.

Deyoe EA, Bandettini P, Neitz J, Miller D, Winans P. Functional magnetic resonance imaging (FMRI) of the human brain. J.Neurosci.Methods. 1994; 54:171–187. [PubMed: 7869750]

French JA, Kenny D, Scott JP, Hoffmann RG, Wood JD, Hudetz AG, Hillery CA. Mechanisms of stroke in sickle cell disease: sickle erythrocytes decrease cerebral blood flow in rats after nitric oxide synthase inhibition. Blood. 1997; 89:4591–4599. [PubMed: 9192784]

Friston KJ, Fletcher P, Josephs O, Holmes A, Rugg MD, Turner R. Eventrelated fMRI: characterizing differential responses. Neuroimage. 1998; 7:30–40. [PubMed: 9500830]

Gajjar A, Chintagumpala M, Ashley D, Kellie S, Kun LE, Merchant TE, Woo S, Wheeler G, Ahern V, Krasin MJ, Fouladi M, Broniscer A, Krance R, Hale GA, Stewart CF, Dauser R, Sanford RA, Fuller C, Lau C, Boyett JM, Wallace D, Gilbertson RJ. Risk-adapted craniospinal radiotherapy followed by high-dose chemotherapy and stem-cell rescue in children with newly diagnosed medulloblastoma (St Jude Medulloblastoma-96): long-term results from a prospective, multicentre trial. Lancet Oncol. 2006; 7:813–820. [PubMed: 17012043]

Gibson P, Tong Y, Robinson G, Thompson MC, Currle DS, Eden C, Kranenburg TA, Hogg T, Poppleton H, Martin J, Finkelstein D, Pounds S, Weiss A, Patay Z, Scoggins M, Ogg R, Pei Y, Yang ZJ, Brun S, Lee Y, Zindy F, Lindsey JC, Taketo MM, Boop FA, Sanford RA, Gajjar A, Clifford SC, Roussel MF, McKinnon PJ, Gutmann DH, Ellison DW, Wechsler-Reya R, Gilbertson RJ. Subtypes of medulloblastoma have distinct developmental origins. Nature. 2010; 468:1095–1099. [PubMed: 21150899]

Gustard S, Williams EJ, Hall LD, Pickard JD, Carpenter TA. Influence of baseline hematocrit on between-subject BOLD signal change using gradient echo and asymmetric spin echo EPI. Magn Reson Imaging. 2003; 21:599–607. [PubMed: 12915190]

Heeney MM, Ware RE. Hydroxyurea for children with sickle cell disease. Pediatr.Clin.North Am. 2008; 55:483–501. x. [PubMed: 18381097]

Helton KJ, Paydar A, Glass J, Weirich EM, Hankins J, Li CS, Smeltzer MP, Wang WC, Ware RE, Ogg RJ. Arterial spin-labeled perfusion combined with segmentation techniques to evaluate cerebral blood flow in white and gray matter of children with sickle cell anemia. Pediatr.Blood Cancer. 2009; 52:85–91. [PubMed: 18937311]

Hogan AM, Pit-ten C, I, Vargha-Khadem F, Prengler M, Kirkham FJ. Physiological correlates of intellectual function in children with sickle cell disease: hypoxaemia, hyperaemia and brain infarction. Dev.Sci. 2006; 9:379–387. [PubMed: 16764611]

Kastrup A, Li TQ, Kruger G, Glover GH, Moseley ME. Relationship between cerebral blood flow changes during visual stimulation and baseline flow levels investigated with functional MRI. Neuroreport. 1999; 10:1751–1756. [PubMed: 10501569]

Leontiev O, Buxton RB. Reproducibility of BOLD, perfusion, and CMRO2 measurements with calibrated-BOLD fMRI. Neuroimage. 2007; 35:175–184. [PubMed: 17208013]

Levin JM, Frederick BB, Ross MH, Fox JF, von Rosenberg HL, Kaufman MJ, Lange N, Mendelson JH, Cohen BM, Renshaw PF. Influence of baseline hematocrit and hemodilution on BOLD fMRI activation. Magn Reson.Imaging. 2001; 19:1055–1062. [PubMed: 11711229]

Luh WM, Wong EC, Bandettini PA, Hyde JS. QUIPSS II with thin-slice TI1 periodic saturation: a method for improving accuracy of quantitative perfusion imaging using pulsed arterial spin labeling. Magn Reson.Med. 1999; 41:1246–1254. [PubMed: 10371458]

Manci, E.; Culberson, D.; Tucker, A. Vasculopathy of sickle cell disease. 9 ed. 1996. p. 4P

Mandeville JB, Marota JJ, Kosofsky BE, Keltner JR, Weissleder R, Rosen BR, Weisskoff RM. Dynamic functional imaging of relative cerebral blood volume during rat forepaw stimulation. Magn Reson.Med. 1998; 39:615–624. [PubMed: 9543424]

Moore CI, Cao R. The hemo-neural hypothesis: on the role of blood flow in information processing. J.Neurophysiol. 2008; 99:2035–2047. [PubMed: 17913979]

Morris EB, Phillips NS, Laningham FH, Patay Z, Gajjar A, Wallace D, Boop F, Sanford R, Ness KK, Ogg RJ. Proximal dentatothalamocortical tract involvement in posterior fossa syndrome. Brain. 2009; 132:3087–3095. [PubMed: 19805491]

Mulhern RK, Merchant TE, Gajjar A, Reddick WE, Kun LE. Late neurocognitive sequelae in survivors of brain tumours in childhood. Lancet Oncol. 2004; 5:399–408. [PubMed: 15231246]

Mumford JA, Hernandez-Garcia L, Lee GR, Nichols TE. Estimation efficiency and statistical power in arterial spin labeling fMRI. Neuroimage. 2006; 33:103–114. [PubMed: 16860577]

Ogawa S, Lee TM, Kay AR, Tank DW. Brain magnetic resonance imaging with contrast dependent on blood oxygenation. Proc.Natl.Acad.Sci.U.S.A. 1990; 87:9868–9872. [PubMed: 2124706]

Oguz KK, Golay X, Pizzini FB, Freer CA, Winrow N, Ichord R, Casella JF, van Zijl PC, Melhem ER. Sickle cell disease: continuous arterial spin-labeling perfusion MR imaging in children. Radiology. 2003; 227:567–574. [PubMed: 12663827]

Ohm JE, Carbone DP. Immune dysfunction in cancer patients. Oncology (Williston.Park). 2002; 16:11–18. [PubMed: 11829278]

Pauling L, Coryell CD. The Magnetic Properties and Structure of Hemoglobin, Oxyhemoglobin and Carbonmonoxyhemoglobin. Proc.Natl.Acad.Sci.U.S.A. 1936; 22:210–216. [PubMed: 16577697]

Prohovnik I, Hurlet-Jensen A, Adams R, De VD, Pavlakis SG. Hemodynamic etiology of elevated flow velocity and stroke in sickle-cell disease. J.Cereb.Blood Flow Metab. 2009; 29:803–10. [PubMed: 19209182]

Reiter CD, Wang X, Tanus-Santos JE, Hogg N, Cannon RO, III, Schechter AN, Gladwin MT. Cell-free hemoglobin limits nitric oxide bioavailability in sicklecell disease. Nat.Med. 2002; 8:1383–1389. [PubMed: 12426562]

Salsman VS, Chow KK, Shaffer DR, Kadikoy H, Li XN, Gerken C, Perlaky L, Metelitsa LS, Gao X, Bhattacharjee M, Hirschi K, Heslop HE, Gottschalk S, Ahmed N. Crosstalk between medulloblastoma cells and endothelium triggers a strong chemotactic signal recruiting T lymphocytes to the tumor microenvironment. PLoS.One. 2011; 6:e20267. [PubMed: 21647415]

Schatz J, White DA, Moinuddin A, Armstrong M, DeBaun MR. Lesion burden and cognitive morbidity in children with sickle cell disease. J.Child Neurol. 2002; 17:891–895. [PubMed: 12593461]

Steen RG, Langston JW, Ogg RJ, Manci E, Mulhern RK, Wang W. Ectasia of the basilar artery in children with sickle cell disease: Relationship to hematocrit and psychometric measures. J.Stroke Cerebrovasc.Dis. 1998a; 7:32–43. [PubMed: 17895054]

Steen RG, Reddick WE, Glass JO, Wang WC. Evidence of cranial artery ectasia in sickle cell disease patients with ectasia of the basilar artery. J.Stroke Cerebrovasc.Dis. 1998b; 7:330–338. [PubMed: 17895109]

Steen RG, Xiong X, Langston JW, Helton KJ. Brain injury in children with sickle cell disease: prevalence and etiology. Ann.Neurol. 2003; 54:564–572. [PubMed: 14595645]

Strouse JJ, Cox CS, Melhem ER, Lu H, Kraut MA, Razumovsky A, Yohay K, van Zijl PC, Casella JF. Inverse correlation between cerebral blood flow measured by continuous arterial spin-labeling (CASL) MRI and neurocognitive function in children with sickle cell anemia (SCA). Blood. 2006; 108:379–381. [PubMed: 16537809]

Vichinsky EP, Neumayr LD, Gold JI, Weiner MW, Rule RR, Truran D, Kasten J, Eggleston B, Kesler K, McMahon L, Orringer EP, Harrington T, Kalinyak K, De Castro LM, Kutlar A, Rutherford CJ, Johnson C, Bessman JD, Jordan LB, Armstrong FD. Neuropsychological dysfunction and neuroimaging abnormalities in neurologically intact adults with sickle cell anemia. JAMA. 2010; 303:1823–1831. [PubMed: 20460621]

Wang W, Enos L, Gallagher D, Thompson R, Guarini L, Vichinsky E, Wright E, Zimmerman R, Armstrong FD. Neuropsychologic performance in school-aged children with sickle cell disease: a report from the Cooperative Study of Sickle Cell Disease. J.Pediatr. 2001; 139:391–397. [PubMed: 11562619]

Ware RE, Steinberg MH, Kinney TR. Hydroxyurea: an alternative to transfusion therapy for stroke in sickle cell anemia. Am.J.Hematol. 1995; 50:140–143. [PubMed: 7572993]

Ware RE, Zimmerman SA, Schultz WH. Hydroxyurea as an alternative to blood transfusions for the prevention of recurrent stroke in children with sickle cell disease. Blood. 1999; 94:3022–3026. [PubMed: 10556185]

Wechsler, D. Wechsler Abbreviated Scale of Intelligence (WASI). San Antonio, TX: Harcourt Assessment; 1999.

Wong EC, Buxton RB, Frank LR. Implementation of quantitative perfusion imaging techniques for functional brain mapping using pulsed arterial spin labeling. NMR Biomed. 1997; 10:237–249. [PubMed: 9430354]

Zou P, Mulhern RK, Butler RW, Li CS, Langston JW, Ogg RJ. BOLD responses to visual stimulation in survivors of childhood cancer. Neuroimage. 2005; 24:61–69. [PubMed: 15588597]

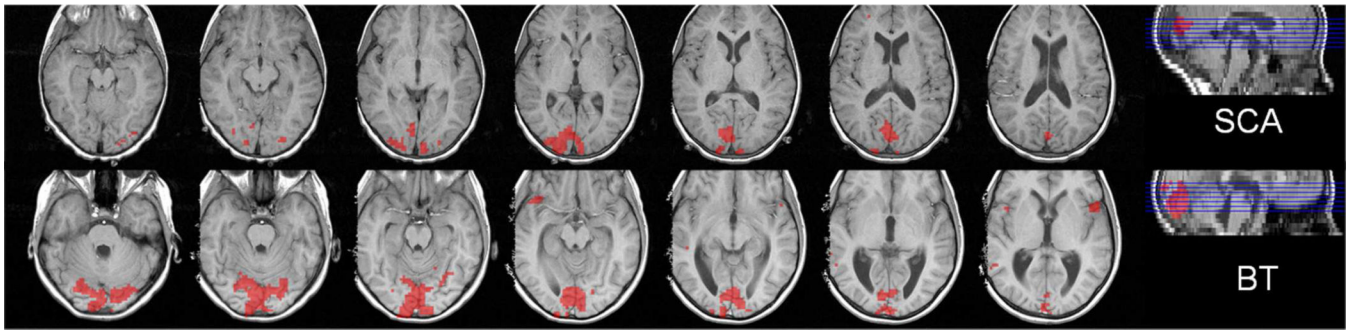


**Figure 1.**
Representative map of brain activation during the visual stimulation paradigm (the standard BOLD measurement) for the SCA (upper row) and brain tumor control (lower row) patients, who had the median activation volume in the corresponding group. The activation volume was significantly smaller in the SCA patient than the control patient (activation thresholds: $p = 0.001$ and $k = 5$).

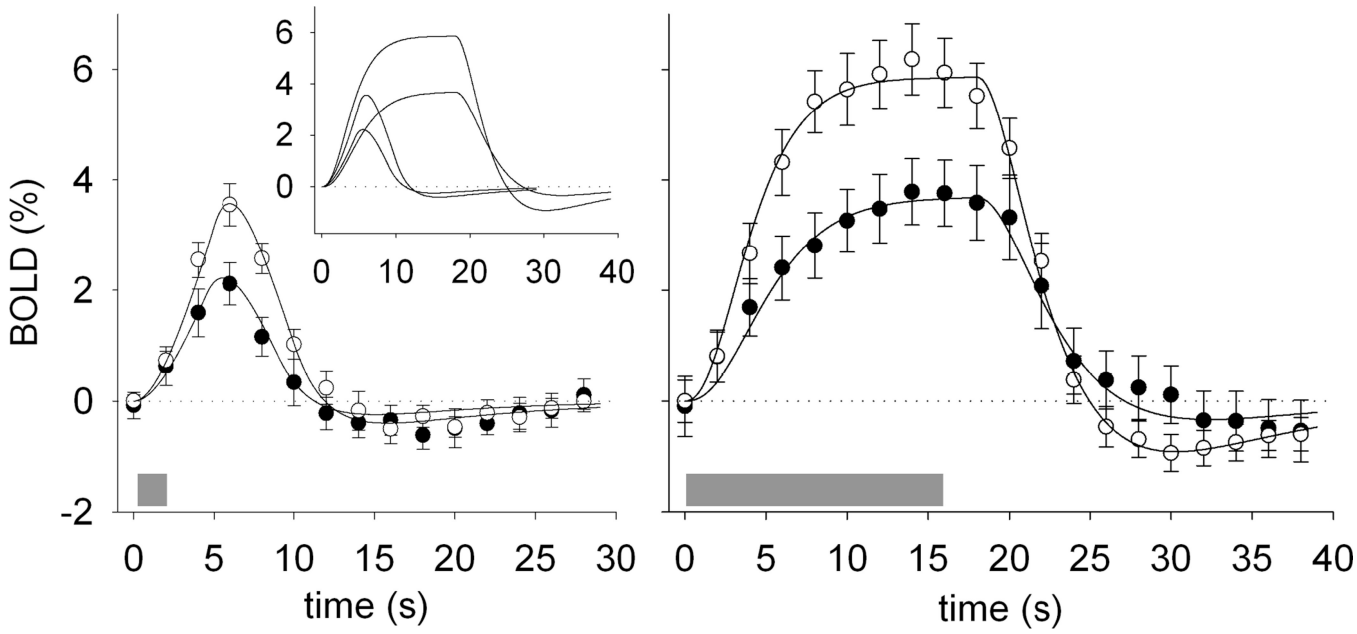


**Figure 2.**

BOLD responses to visual stimulation were diminished in children with SCA. The amplitude of the BOLD response to 2-s (left) and 16-s (center) visual stimulation was significantly lower in SCA patients (black circles) than in control patients (white circles) patients. The gray bars indicate the time of the visual stimulation, and the error bars show the standard error of the mean across subjects in each group. The solid curves in each plot are Balloon Model (Buxton et al., 2004) fits to approximate the BOLD responses for each condition Parameters for the 16 s stimulus are shown in the Table 2. The stimulation paradigm had four 30 s blocks in which stimulus was on for 2 s and three 40 s blocks in which the stimulus was on for 16 s. The small inset graph in the left panel shows the balloon model results for the short and long stimulus together and demonstrates the consistency of the BOLD response features across the conditions.

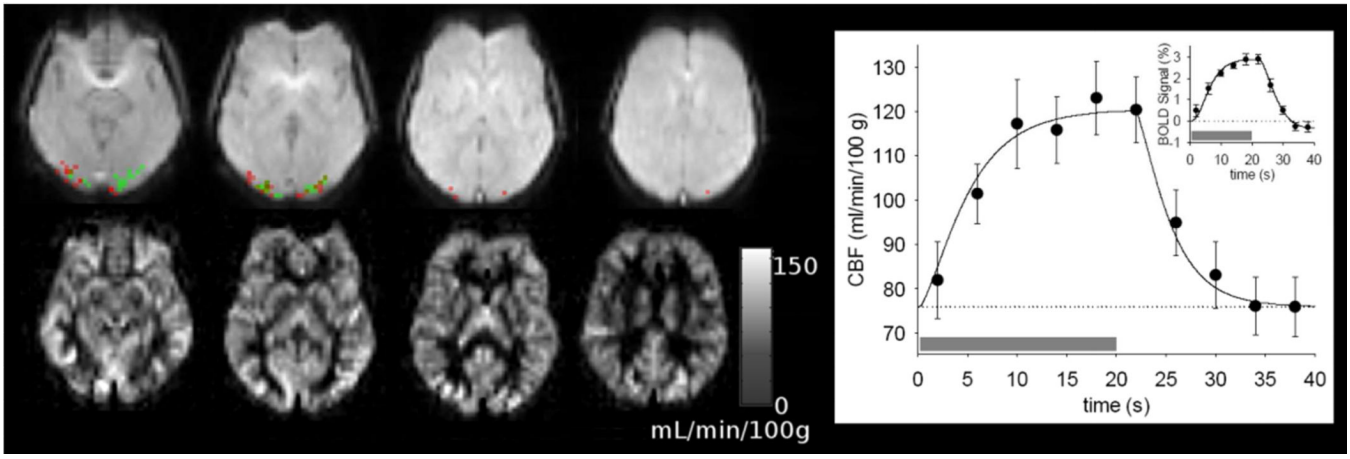


**Figure 3.**

CBF and visual activation detected with the ASL measurement for the SCA patient with the median activation volume. The images in the lower row are maps of baseline perfusion calculated from the ASL data. Images in the upper row show activation in the visual cortex detected by CBF change (green) and BOLD signal change (red) during stimulation. The graph on the right shows average CBF response to visual stimulation measured with ASL in SCA patients. The gray bars indicate the time of the visual stimulation, and the error bars show the standard error of the mean across the group. The solid curve in the CBF plot is a numerical approximation generated by filtering a rectangular function (supplementary online material). The small inset graph shows the BOLD response to visual stimulation estimated from the ASL data. The solid curve in BOLD signal plot is the Balloon Model fit to approximate the BOLD response. The stimulation paradigm had eight 40 s blocks with stimulus on for 20 s.

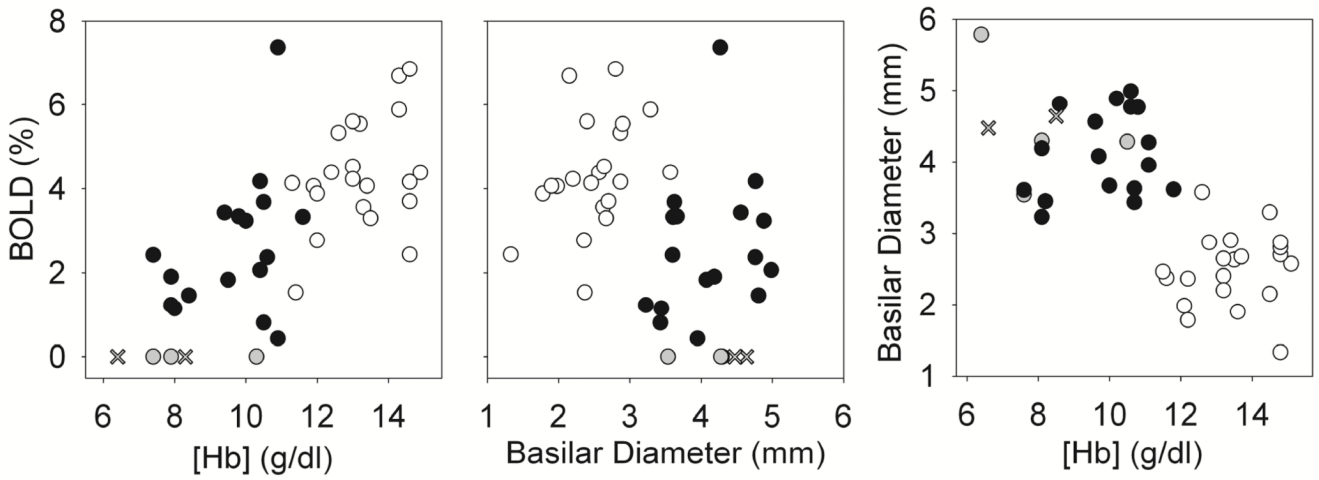


**Figure 4.**

The BOLD response and hematologic variables. The BOLD signal amplitude was significantly associated with both [Hb] ($r_s = 0.71$, $p < 0.00001$) and basilar artery diameter ($r_s = -0.44$, $p = 0.004$). Basilar artery diameter, an index of cerebral blood volume, was also inversely associated with [Hb] ($r_s = -0.69$, $p < 0.00001$). SCA patients with detectable activation are indicated by black circles and control patients are indicated by white circles. The SCA patients without detectable activation are shown with gray circles, and × indicates the two patients who were not on hydroxyurea therapy. Graphs show the responses for the 2 s stimulus. Responses for the 16 s stimulus (not shown) were essentially the same as those shown for the 2 s stimulus. $r_s$: Spearman's correlation coefficient.

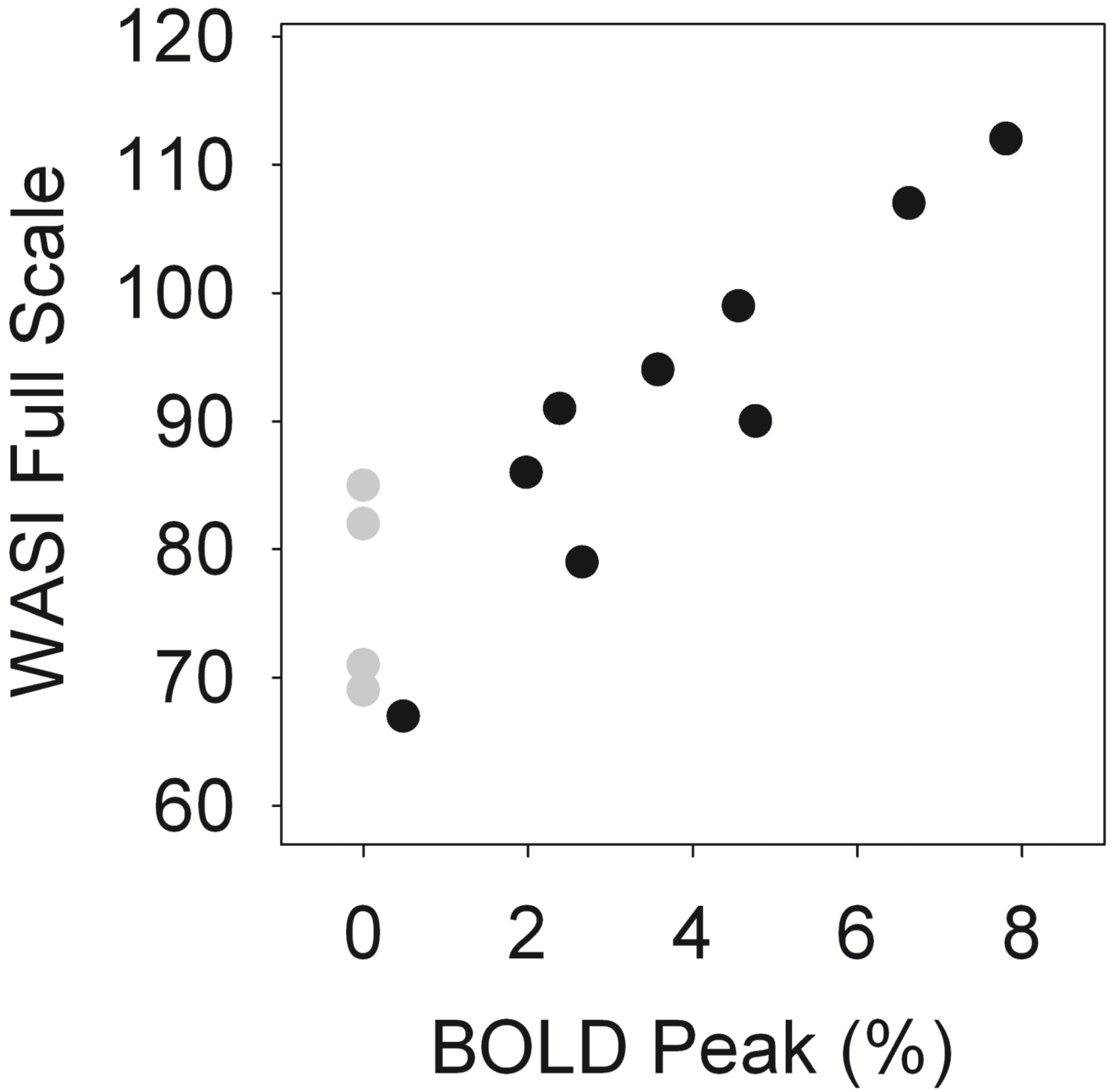


**Figure 5.**
WASI Full-Scale score was strongly associated the BOLD response to visual stimulation in the patients with SCA ($r_s$ = 0.81). The filled symbols indicate the BOLD signal for the 16 s stimulus. SCA patients with detectable BOLD activation (n = 9) and the gray symbols indicate SCA patients without detectable BOLD activation (n = 4). Graphs for the 2 s stimulus (not shown) were essentially the same as those shown for the 16 s stimulus. $r_s$: Spearman's correlation coefficient

## Table 1

Clinical, Imaging, and Psychometric Variables for SCA and Control Patients.

| | | SCA [n=23] | Control [n=21] | Significant |
|---|---|---|---|---|
| *Clinical (1)* | Age (years) | 12.6 (5.3, 17.9) | 11.7 (6.2, 19.7) | N |
| | Hb (g/dl) | 9.5 (6.2, 11.2) | 13.2(11.3, 14.9) | P=0.0003 |
| | HbF (%) | 15 (2, 33) [n=22] | -- | -- |
| | ABS Retic. ($\times 10^6/\mu L$) | 0.16 (0.06, 0.42) [n=22] | -- | -- |
| | ACS Events | 2 (0, 4) [n=22] | -- | -- |
| | TCD in MCA (cm/sec) | 124 (83, 184) [n=20] | -- | -- |
| *Anatomic imaging(2)* | Basilar Art. Diam. (mm) | 4.3 (3.2, 5.8) | 2.6 (1.3, 3.6) | p=0.0003 |
| *Standard BOLD (3)* | BOLD_2s (%) | 2.36 (0.43, 7.37) | 4.16 (1.53, 6.86) | p=0.0006 |
| | BOLD_16s (%) | 2.81 (0.10, 7.83) | 6.88 (1.99, 11.57) | p=0.02 |
| | Activated Volume ($cm^3$) | 5.50 (0.23, 20.2) | 19.08 (1.31, 48.51) | p=0.0003 |
| *CBF(ml/min/100g) (4) [n=22, SCA only]* | Whole Brain Gray Matter | 84.5 (23.8,117.2) | -- | -- |
| | Whole Brain White Matter | 38.0 (11.5, 69.9) | -- | -- |
| | Occipital Gray Matter | 92.3 (26.6, 150.8) | -- | -- |
| | Occipital White Matter | 49.6 (15.0, 92.9) | -- | -- |
| *WASI (5) [n=13, SCA only]* | Full Scale | 86 (67, 112) | -- | -- |
| | Performance | 88 (59, 106) | -- | -- |
| | Verbal | 85 (70, 119) | -- | -- |

Note: All values in the table are presented in format *median (min, max),* and .n. in the square brackets indicates the number of subjects with available data if less than 23 for SCA or 21 for brain tumor control. The Wilcoxon-Mann-Whitney Test was used for group differences, and the Holm.s procedure was used to adjust p-values for multiple comparisons. Only significant p-values after adjustment are shown.

*(1)*Hb: Hemoglobin concentration, normal range 11 – 16 g/dl for children; HbF: Fetal Hemoglobin, hydroxyurea therapy increases the HbF levels in patients with SCA; ABS Retic: Absolute Reticulocyte count, normal range 0.05 $\times 10^6$ to 0.15$\times 10^6/\mu L$; ACS events: number of acute chest syndrome events, a complication of SCA; and TCD in MCA: transcranial Doppler of blood flow in the middle cerebral artery, normal ≤ 170 cm/sec, conditional 171 to 200 cm/sec, and abnormal ≥ 200 cm/sec.

*(2)*Basilar Art. Diam: Basilar artery diameter, an index for CBV (Steen et al., 1998a).

*(3)*Peak percent BOLD signal changes (BOLD_2s (%) and BOLD_16s (%)) and activated volume were measured with the standard BOLD fMRI pulse sequence. _2s and _16s indicate visual stimulus duration of 2 s and 16 s, respectively. Results summarize responses from the 17 out of 23 of SCA patients and all the 21 brain tumor controls with detectable visual cortex activation.

*(4)*The CBF values of 22 SCA patients were measured with the ASL Q2TIPS pulse sequence (Luh et al., 1999).

*(5)*Wechsler Abbreviates Scale of Intelligence (WASI) scores (mean 100, SD = 15), an indication of global cognitive function, were below average in the 13 SCA patients.

**Table 2**

Balloon model parameters for SCA patients and Control Patients

| Parameter | Group Average Model | | Individual Models | |
|---|---|---|---|---|
| | Control | SCA | Control | SCA |
| $V_0$ | 0.04 | 0.06 | 0.04 (0.021, 0.051) | 0.06 (0.045, 0.070) |
| rHb | 1.00 | 0.76 | 1.00 (0.86, 1.13) | 0.76 (0.56, 0.89) |
| $\Delta E/E_0$ | 0.36 | 0.26 | 0.35 (0.21, 0.52) | 0.25 (0.14, 0.34) |
| $\Delta f$ | 0.85 | 0.62 | 0.85 (0.51, 1.50) | 0.60 (0.39, 0.83) |
| $\alpha$ | 0.40 | 0.48 | 0.40 (0.1, 0.5) | 0.48 (0, 0.65) |
| $\tau$ | 2 | 3 | 2 (1.0, 4.0) | 3 (2.0, 4.2) |
| $\tau_+$ | 10 | 8 | 10 (3, 25) | 9 (3.5, 30) |
| $\tau_-$ | 20 | 12 | 20 (10, 40) | 17 (1, 40) |

Notes: $V_0$: fractional blood volume; rHgb: relative blood hemoglobin concentration; E0: baseline oxygen extraction fraction, $\Delta E$: oxygen extraction fraction change during activation; $\Delta f$: fractional CBF change during activation; $\alpha$: Flow-volume relationship; $\tau$: mean transit time; $\tau+$: vascular balloon inflation time-constant; $\tau-$: vascular balloon deflation time-constant (see supplementary online material for details of the modeling).

## Table 3

Hematologic Parameters for SCA Patients with and without Detectable BOLD Activation in Visual Cortex during Visual Stimulation

| SCD cohort [N=23] | With Activation | Without Activation | p value |
|---|---|---|---|
| Hb (g/dl) | 10 (7.4, 11.6) [n=17] | 7.6 (6.2, 10.3) [n=6] | p = 0.01 |
| HbF (%) | 20.7 (5.8, 32.6) [n=17] | 3.9 (2.1, 21.3) [n=5] | p = 0.03 |
| ABS Retic. ($\times 10^6/\mu L$) | 0.14 (0.06, 0.28) [n=17] | 0.21 (0.17, 0.42) [n=5] | p = 0.01 |

Note: Median values are listed with minimum and maximum in parentheses. N is the total number of SCA patients and n indicates the number of subjects with available data in each subgroup. The Wilcoxon-Mann-Whitney test was used for group difference, and Holm.s procedure was used to adjust p-values for multiple comparisons. Other clinical parameters with no significant difference between the groups of SCA patients are not shown.